



# Circulations Associated with Variations in Boreal Spring Rainfall over Kenya

Brian Odhiambo Ayugi<sup>1</sup> · Guirong Tan<sup>1</sup> · Victor Ongoma<sup>1,2</sup> · Kantamla Biseke Mafuru<sup>1,3</sup>

Received: 24 December 2017 / Accepted: 7 September 2018  
© Springer Nature Switzerland AG 2018

## Abstract

The decline in March–May (MAM) ‘boreal spring’ rainfall is of great concern to Kenya’s agricultural sector. This study examines factors influencing MAM rainfall variability based on monthly observed and Climatic Research Unit (CRU) reanalysis rainfall datasets for the period 1971–2010. The distribution patterns of MAM rainfall were analyzed using Empirical Orthogonal Functions (EOF), whereas the Sequential Mann–Kendall (MK) statistic was used for trend analysis. Factors influencing seasonal rainfall were determined and assessment of the circulation anomalies associated with wet/dry condition during the study period was carried out. The MAM rainfall revealed decreasing trend. Wet years are associated with enhanced low-level convergence and upper-level divergence of winds, advection of moisture flux following a well-positioned and intensified Arabian high-pressure cell, and an accompanying rising branch of Walker circulation over Indian Ocean (IO). The sea surface temperatures anomalies (SSTAs) in the central and sub-tropical IO are closely related to MAM rainfall over Kenya. Positive SSTAs accompanying negative OLR anomalies may lead to intensified rising branch of the Walker circulation influencing the MAM wet events in Kenya. There is a negative correlation coefficient of  $-0.62$  between MAM rainfall and Outgoing Long-wave Radiation (OLR) indicating that the inter-annual variation of the MAM rainfall and OLR are in opposing phases and, hence, more convection and enhanced rainfall over the study domain. The study reveals that the circulation anomalies associated with the dry years are opposite to those in wet years, forming a good basis of monitoring similar events in future.

**Keywords** Rainfall variability · Trend analysis · Circulation anomalies · Kenya

## 1 Introduction

The Kenyan population is mainly dependent on rain fed agriculture (Brass and Jolly 1993; Ministry of Agriculture 2009) and, as a result, they are highly vulnerable to effects of climate variability and change. An increase in evapotranspiration associated with surface warming leads to an increase in

drying trend and decreasing the number of growing-seasons days (Cook and Vizy 2013; Marshall et al. 2012). There is a need, therefore, to understand the past and current trends of rainfall events and influencing factors in the effort of making long-term projections since rainfall patterns over East Africa (EA) exhibit pronounced regional variations with complex seasonal cycles (Cook and Vizy 2013).

A number of studies have investigated temporal variability of rainfall over EA (Indeje et al. 2000; Nicholson and Selato 2000; Nicholson et al. 2001; Camberlin et al. 2001; Black et al. 2003, 2015; Clark et al. 2003; Ogwang et al. 2014; Yang et al. 2015a; Ayugi et al. 2016; Ongoma and Chen 2017). Though some studies are involved in both the ‘boreal spring’ rainfall during March–May (MAM) as ‘long rains’, and ‘boreal fall’ during October–December (OND) as ‘short rains’, most of the studies focus on the variability of MAM rainfall since it significantly influences growing seasons over Eastern Ethiopia, Somalia, Southern Kenya, Eastern Uganda and much of Tanzania (e.g., Cook and Vizy

✉ Brian Odhiambo Ayugi  
ayugibrian@outlook.com

<sup>1</sup> Key Laboratory of Meteorological Disaster, Collaborative Innovation Center on Forecast and Evaluation of Meteorological Disasters, Ministry of Education, Nanjing University of Information Science and Technology, Nanjing 210044, China

<sup>2</sup> Department of Meteorology, South Eastern Kenya University, P.O. Box 170-90200, Kitui, Kenya

<sup>3</sup> Tanzania Meteorological Agency, P. O. Box 3056, Dar es Salaam, Tanzania

2013). These studies have unraveled a number of factors that influence variability, trends and periodicities of rainfall over the region. These factors include Inter-Tropical Convergence Zone (ITCZ), monsoon winds, sub-tropical high-pressure systems, Easterly/Westerly waves, El Nino Southern Oscillation (ENSO), Quasi Biennial Oscillation (QBO), and Indian Ocean Dipole (IOD) (Manatsa et al. 2014; Ogwang et al. 2015a). These factors are associated with extreme rainfall that results in floods or droughts over the region (Camberlin and Okoola 2003). For example, Nicholson (2016) reported that EA's seasonal rainfall is generally linked to the relative stability of the northeasterly and southeasterly trade wind regimes and the ITCZ plays a big role in the distribution and variability of rainfall patterns over the study area.

According to studies (Owiti et al. 2008; Maidment et al. 2015), the Indian Ocean is reported to have a significant and direct impact that influences the East African rainfall as compared to other oceans. Both the MAM and OND rainfall seasons are normally associated with solar heating maxima during the equinox (Daron 2014). Factors such as the sea surface temperature (SST) and Indian monsoon also influence the timing and intensity of the seasonal rainfall (Okoola 1999; Hastenrath et al. 2011; Ogwang et al. 2014).

Recent findings by Liebmann et al. (2014) suggest that the decrease in MAM could be due to an increased zonal gradient in SST between Indonesia and the central Pacific. This is in agreement with the observations made by Funk et al. (2014) on climatic conditions associated with drying trends in the western central Pacific and central Indian

Ocean that reoccurs during the MAM. However, other studies (e.g., Indeje et al. 2000 and Ogwang et al. 2014) showed that the long rainfall in MAM is dominated by local factors rather than the large-scale factors in regulating variability of rainfall. In contrast, the OND rainfall has been observed to increase and is projected to continue increasing to the end of twenty-first century (Ongoma and Chen 2017; Ongoma et al. 2018a), mostly due to Western Indian Ocean (WIO) warming (Liebmann et al. 2014).

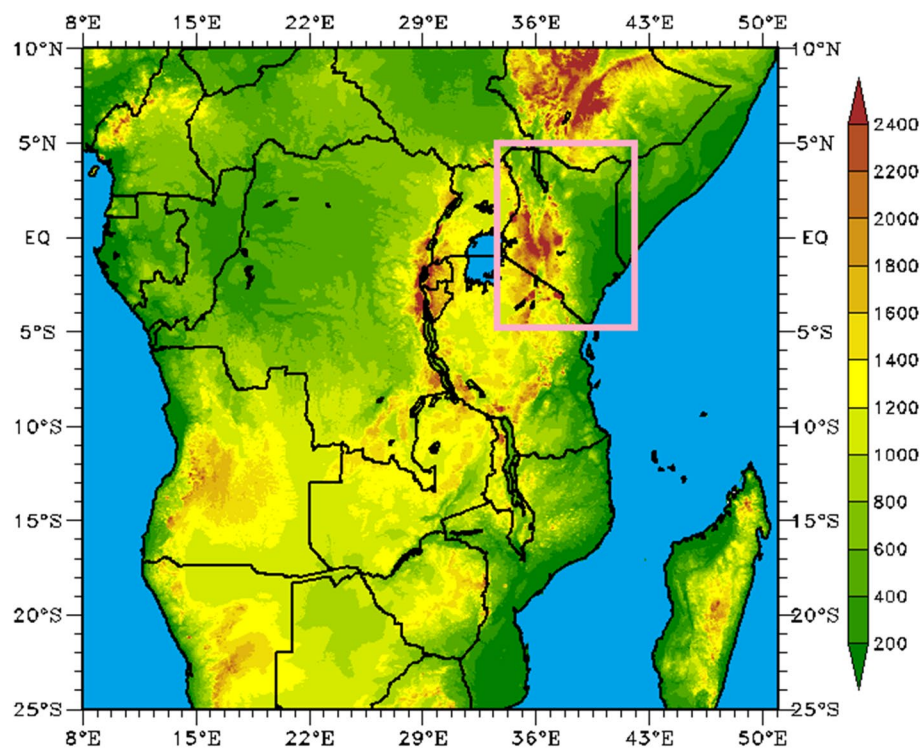
The aim of this paper is to investigate the circulations associated with MAM rainfall variability over Kenya and to understand the mechanisms of the recent drying variation. The outcome of this work is important to climate forecasters in monitoring similar events in future. This could help farmers and other climate users to plan and adapt to variability and changes in climate. The remaining part of the paper is structured as follows: Sect. 2 gives data and methodology while Sect. 3 presents the results and discussion. The conclusion and recommendations drawn from the findings are summarized in Sect. 4.

## 2 Data and Methodology

### 2.1 Study Area

The map of Kenya is shown in (Fig. 1). It is located in EA along Indian Ocean coast between Somalia and Tanzania, bound within longitude 34°E–42°E and latitude 5°S–5°N.

**Fig. 1** Topographical elevation (m) of Kenya, 34°E–42°E and 5°S–5°N [Orange Rectangle]



The country's total land coverage is 582,650 km<sup>2</sup>, with land covering about 569,140 km<sup>2</sup> (Bowden 2007). Kenya has a diverse geography with a coastline bordering Indian Ocean that contains swamps of East African mangroves while inland are broad plains and numerous hills. The Central and Western Kenya is characterized by vast rift valley. Mt. Elgon is on the border between Western Kenya and Uganda. The highest elevation point is Kenya's highest mountain located in central parts of the country reaching over 5000 m in height.

Most parts of the country receive bimodal rainfall patterns with 'long rains' season experienced in MAM and 'short rains' observed in OND (Fig. 2). This has been observed in the past studies (Indeje et al. 2000; Maidment et al. 2015; Yang et al. 2015; Ayugi et al. 2016; Boiyo et al. 2016). Movement of ITCZ has been identified to be the main source of influence of the observed rainfall seasonality (Nicholson 2008). These seasons are also associated with maximum solar heating during the overhead sun over the equator (Camberlin and Okoola 2003; Yang et al. 2014; Ongoma and Chen 2017).

The country is generally characterized by warm temperature throughout the year, with slight variations from one season to another (Ongoma et al. 2017). Kenya is defined as a tropical savanna climate (Aw) (Peel et al. 2007). Mean annual temperature over the study region ranges between 19 and 30 °C. The warmest months are January and February (JF), followed by MAM season, while June–September (JJAS) records the lowest temperatures (King'uyu et al. 2000; Schreck and Semazzi 2004; Ongoma et al. 2017; Kerandi et al. 2018). The cold zone is generally in the areas at high elevation, on either side of the Rift Valley. In support of the elevation effect on temperature, low temperatures are observed near the central and Rift Valley regions. The eastern and northwestern parts of the country record the highest temperatures since the areas are mainly Arid- and Semi-Arid Lands (ASAL), characterized by low rainfall. The northeasterly winds prevail during the JF and JJAS seasons, while the south easterlies are dominant during MAM and OND (Hastenrath et al. 2011).

## 2.2 Data

The study utilized monthly rain gauge observations provided by the Kenya Meteorological Department (KMD). The data can be accessed via online link (<http://www.meteo.go.ke/>). The study duration is 40 years, i.e., 1971–2010 (Table 1). Also utilized was monthly Climatic Research Unit (CRU TS 3.22) rainfall data with resolution of 0.5° × 0.5° from University of East Anglia (University of East Anglia 2014). The data have been successfully used in previous research over EA since it performs better as compared to other gridded datasets of the same resolution such as Global Precipitation Climatology Centre (GPCC) (Ogwang et al. 2015b; Ongoma and Chen 2017; Kerandi et al. 2018). The study period was chosen because it encompasses the latest baseline period 1986–2005, adopted by IPCC (2013).

Monthly mean, zonal- and meridional-wind data over the period 1971–2010 were used as potential factors influencing MAM rainfall trend over study region in this study. Winds at 850 hPa (200 hPa) were used because these are linked to low-level (high-level) wind convergence (divergence) that has direct influence on rainfall trends over Kenya and East Africa at large. The data have a resolution of 2.5° × 2.5°. It was obtained from the <http://iridl.ldeo.columbia.edu>. Yang et al. (2015) successfully used the same datasets on study of annual cycle of East African rains.

Version 3b Sea Surface Temperature (SST) data from <http://www.esrl.noaa.gov/psd/> for the same period, 1971–2010, were used. The data have horizontal resolution of 2.5° × 2.5°. Velocity potential and vertical velocity were used to determine the factors influencing trends and periodicities of MAM rainfall. The data are gridded at 2.5° × 2.5° latitude/longitude grid (<http://iridl.ldeo.columbia.edu/>). Gichangi et al. (2015) used the data to determine the associated mechanism responsible for trends and periodicities of MAM rainfall over eastern Kenya. Details of these datasets are summarized in Table 2.

**Fig. 2** Monthly mean variations of meteorological parameters derived from CRU datasets over Kenya (34°E–42°E and 5°S–5°N) for the period 1971–2010. The red color represents temperature (°C), humidity (%) in blue, and rainfall as a bar graph

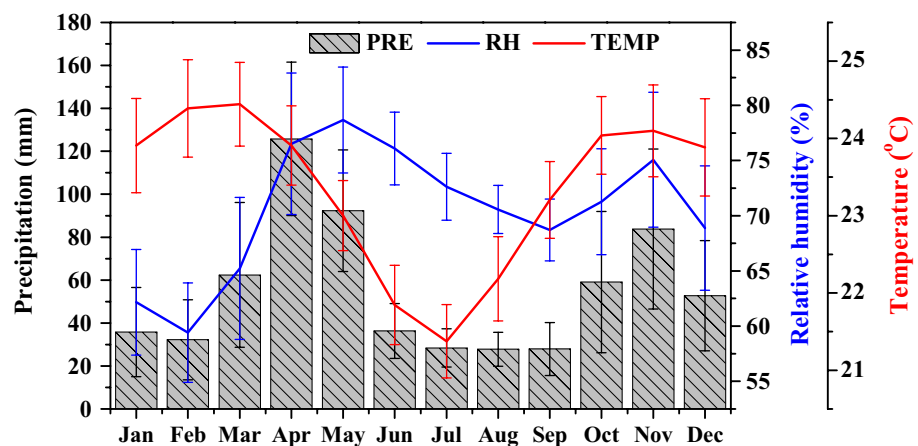


**Table 1** List of synoptic station used in the study and geographical details

No	Station ID	Station name	Longitude	Latitude	Period
1	636860	Eldoret	35.3	0.5	1971–2013
2	183028	Nyahururu	36.4	0	1961–2013
3	637230	Garrissa	39.6	– 0.5	1959–2013
4	636870	Kakamega	34.8	0.3	1958–2013
5	184707	Naivasha	36.4	– 0.8	1961–2013
6	637080	Kisumu	34.8	– 0.1	1959–2013
7	637090	Kisii	34.8	– 0.7	1963–2013
8	179330	Thika	37.1	– 1	1957–2013
9	636120	Lodwar	35.6	3.1	1950–2013
10	637720	Lamu	40.9	– 2.3	1950–2013
11	636240	Mandera	41.9	3.9	1957–2013
12	636410	Marsabit	38	2.3	1950–2013
13	636950	Meru	37.7	0.1	1966–2013
14	637990	Malindi	40	– 3.2	1961–2013
15	638200	Mombasa	39.6	– 4	1957–2013
16	637660	Makindu	37.8	– 2.3	1950–2013
17	636190	Moyale	39.1	3.5	1950–2013
18	637410	Dagoretti	36.7	– 1.3	1955–2013
19	637400	Nairobi JKIA	36.9	– 1.3	1958–2013
20	637170	Nyeri	37	– 0.4	1968–2013
21	637140	Nakuru	36.1	– 0.3	1964–2013
22	637370	Narok	35.9	– 1.1	1950–2013
23	637420	Wilson	36.8	– 1.3	1957–2013
24	636943	Nanyuki	37	– 0.7	1957–2013
25	637930	Voi	38.6	– 3.4	1950–2013
26	636710	Wajir	40.1	1.8	1950–2013

## 2.3 Methodology

Empirical Orthogonal Function (EOF) as described by Lorenz (1956) was used to describe most of the variance in the data by defining dominant mode using eigenvectors. The eigenvector corresponding to the largest eigenvalue of the

covariance matrix is referred to as the leading EOF. The first eigenvector points to the direction in which the data vectors jointly exhibit the most variability. The eigenvector associated with the second largest eigenvalue of the covariance matrix is referred to as the second EOF. This structure is uncorrelated with the other structures and is orthogonal to the first eigenvector, which is orthogonal to the third eigenvector and so on. The eigenvector with the highest Eigen value is the first principal component (PC) of the dataset and has similar weights on each grid square. In this study, the analysis of EOF was aimed at determining the dominant mode responsible for MAM rainfall over Kenya. The modes that account for the largest percent of the original variability are considered significant. These modes were represented by orthogonal spatial patterns (eigenvectors) and corresponding time series (principal components). The composite analysis, previously used by a number of studies (Okoola 1999; Stern et al. 2011; Mouhamed et al. 2013; Ogwang et al. 2014), was used to identify and average one or more categories of fields of a variable selected according to their association with key conditions. The wet (flood) and dry (drought) years used were identified using Standard Precipitation Index (SPI) guide and following the recommendations by Makkonen, (2006) on exceeding standard deviation of  $\pm 1$ . The wet and dry are events/years whose normalized standard deviation  $\geq 1$  and  $\leq -1$ , respectively. The same categorization was adopted in previous studies over EA (Ogwang et al. 2015b). Composites were separately analyzed especially for winds, velocity potential, vertical velocity, and SST. This was carried out so as to help in identifying the circulation or any anomalies associated with wet/dry years. Student *t* test was applied to determine the probability (*P*) between two variables under study and test the hypothesis on the basis of difference between sample means (Beri 2005).

The detection of abrupt change in MAM rainfall trend was determined using Sequential Mann–Kendall (SQMK) test statistics (Mann 1945; Kendall 1975). The MK test is rank-based non-parametric method used to check existence

**Table 2** Summary of sources and characteristic of data sets used in the present study

Sensor	Parameter	Level	Spatial resolution	Temporal resolution	Duration	Web link
CRU TS 3.22	Precipitation	–	0.5°	Monthly	1971 to 2010	<a href="http://catalogue.ceda.ac.uk/uuid/4a6d071383976a5fb24b5b42e28cf28f">http://catalogue.ceda.ac.uk/uuid/4a6d071383976a5fb24b5b42e28cf28f</a>
ERSST	SST	1	2.5°	Monthly	1971–2010	<a href="http://www.esrl.noaa.gov/psd/">http://www.esrl.noaa.gov/psd/</a>
Global digital elevation model (DEM)	Elevation	–	1 km	–	–	<a href="http://iridl.ldeo.columbia.edu/SOURCES/NOAA/NGDC/GLOBE/topo">http://iridl.ldeo.columbia.edu/SOURCES/NOAA/NGDC/GLOBE/topo</a>
NCEP/NCAR reanalysis	Velocity Potential, Vertical Velocity, U&V and Pressure.	2	2.5°	Monthly	1971–2010	<a href="http://www.esrl.noaa.gov/psd/data/gridded/data.ncep.reanalysis.html">http://www.esrl.noaa.gov/psd/data/gridded/data.ncep.reanalysis.html</a>

of trend in a time series against the null hypothesis of no trend. This MK method is highly recommended for general use by the World Meteorological Organization (WMO) as mentioned in a number of studies (Partal and Kahya 2006; Meng et al. 2013; Bisai et al. 2014; Gajbhiye et al. 2016). This method has been applied widely, especially on climate, environmental and hydrological studies (Araghi et al. 2016; Liuzzo et al. 2016; Ongoma and Chen 2017; Ongoma et al. 2018b). Detailed information regarding the equations for various methods used in this study can be found in a number of studies (Ongoma et al. 2013, 2018b; Ongoma and Chen 2017).

### 3 Results and Discussion

#### 3.1 MAM Rainfall Trends Analysis

A summary of the MAM rainfall trend test using sequential MK statistics is represented in Table 3. The sequential Mann–Kendall test was used to graphically illustrate the forward and backward trends of the MAM rainfall in Kenya for the 1971–2010 climatology (Fig. 3). The overall results reveal no abrupt change; however, decreasing trend in MAM rainfall from 1976 to 2006 was observed. This change was statistically insignificant at the significance levels of 5% significant level. It is worth noting that, in 2006 both the progressive  $u(t)$  and retrogressive  $u'(t)$  lines intersected (Fig. 3) followed by the positive trend towards the end of the climatology. It, therefore, signifies the fact that the abrupt decline in MAM rainfall trend was followed by an increasing trend from 2006 to 2010 which was also insignificant at 95% confidence interval.

These findings are in agreement with other recent studies over larger domain rainfall trends where they observed a general decrease in MAM rainfall (Awange et al. 2007; Camberlin and Okoola 2003; Cook and Vizy 2013; Ongoma et al. 2015; Yang et al. 2014; Ongoma and Chen 2017). Although the OND rainfall has shown a positive trend (Ongoma and Chen 2017), the overall rainfall trend over Kenya is downwards since MAM has a significant influence on total rainfall

**Table 3** A summary of MAM rainfall trend test over Kenya using sequential MK statistics at 5% significant level

Measure	Value
$S$	– 89.000
$Z$	1.0835
Kendall's tau	– 0.120
$P$	0.289
Alpha ( $\alpha$ )	0.05
Significance	Insignificantly decreasing trend

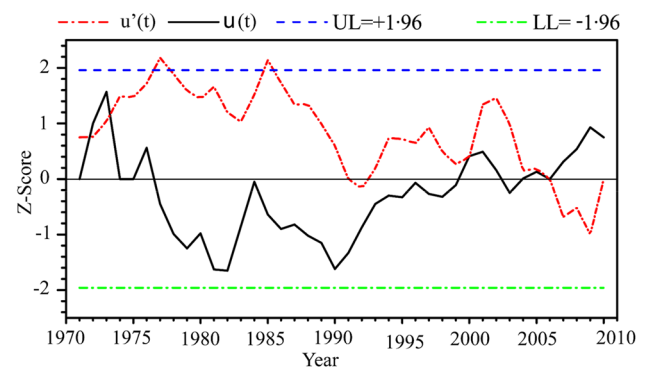


**Fig. 3** The sequential Mann–Kendall trend test in MAM rainfall over Kenya. The  $u(t)$  is forward sequential while  $u'(t)$  is backward sequential based on CRU data. The upper (UL) and lower (LL) dashed lines represent the confidence limits at  $\alpha=5\%$

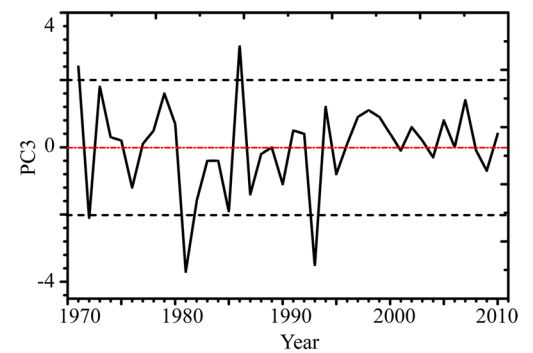
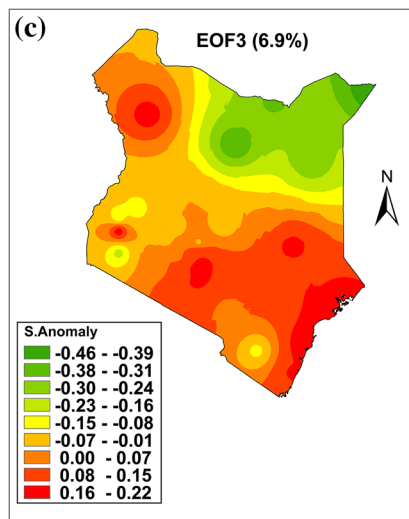
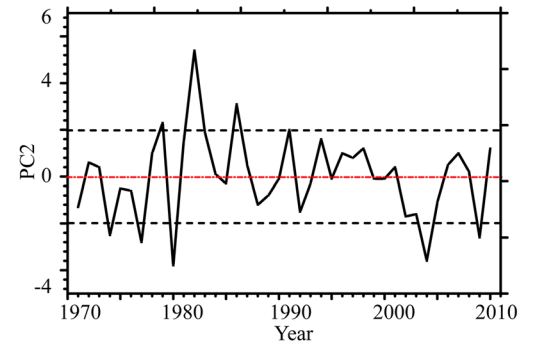
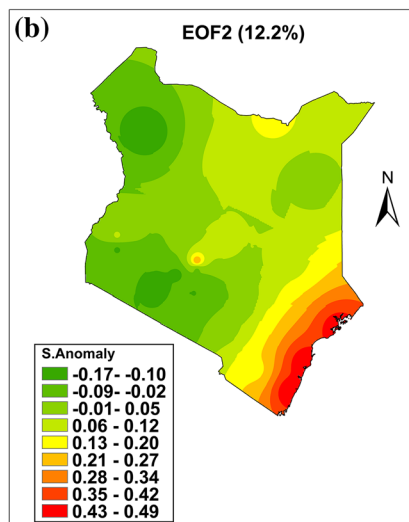
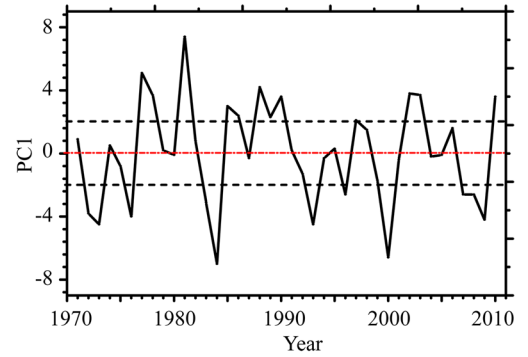
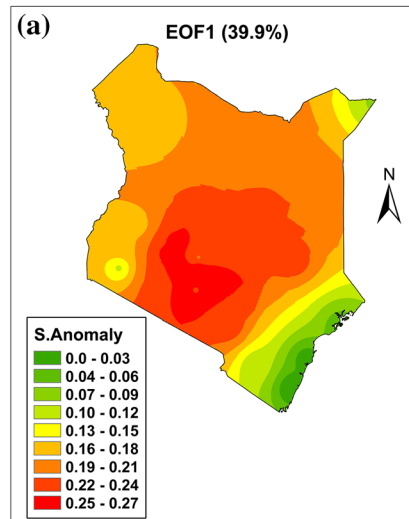
recorded in the entire EA region. This is a great concern since the reduction is likely to negatively affect the economy of Kenya given that most agricultural activities are sustained by MAM rainfall over EA (Ongoma et al. 2018a), which if realized will be a relief on the regions economy.

#### 3.2 Spatial Analysis of MAM rainfall

In this study, EOF analysis was used to investigate the dominant mode of variability of MAM rainfall over study domain. Figure 4 presents the spatial modes and corresponding PCs of the first three EOF modes. The variances that accounted for the first three EOF modes are 39.9%, 12.2% and 6.9%, respectively. Being the dominant mode of variability, the first EOF mode (EOF1) characterizes positive loadings (Fig. 4a) over most parts of the country, denoting consistent variation of the rainfall over these areas. It reflects the likelihood that the central areas being the most affected with anomalous wet conditions than the rest in the study area during MAM season.

The second and third EOF modes (Fig. 4b, c) account for 19.1% of the total variance during MAM rainfall season. The modes display an apparent south–north dipole of positive (negative) loadings (Fig. 4b). EOF3 (Fig. 4c) reveals positive loadings over the north western corner, coastal belt and its hinterlands while the remaining areas favor negative loadings. The PC time series usually provides an insight concerning the strength of an EOF pattern over time (Indeje et al. 2000). Having considered the results obtained from the dominant mode (i.e., EOF1) shows that the amplitudes of greater than one standard deviation were mainly observed in 1977, 1981, 1988, 2002, 2003 and 2010. Similarly, it follows that the amplitudes of less than minus one were observed in 1973, 1976, 1984, 1993, 2000 and 2009. These years were then used in composite analysis to find the possible circulation anomalies that were likely to be associated with the

**Fig. 4** The first three modes for the MAM rainfall showing spatial distribution (Left) and their corresponding principal components (Right) for **a** EOF1, **b** EOF2, and **c** EOF3, over Kenya based on 26 synoptic station data from 1971 to 2010



anomalous wet and dry conditions during the study period. The years and the threshold for anomalous years are summarized in Table 4.

**Table 4** MAM EOF1 for wet/dry years during the period 1971–2010, and the respective standardized anomaly over Kenya (the years with an asterisk (\*) and bold were considered as wet/dry years for further analysis)

EOF Mode	Threshold	Years
EOF 1	2.0 +	<b>1981*</b>
	1.5–1.99	<b>1977*, 1988*, 2002*, 2003*, 2010*</b>
	1.0–1.49	1978, 1985, 1986, 1989,
	1.0 to – 1.49	1990, 1996,
	– 1.5 to – 1.99	1972, 1983, 2007, 2008,
	– 2 and less	<b>1973*, 1976, 1984*, 1993*, 2000*, 2009*</b>

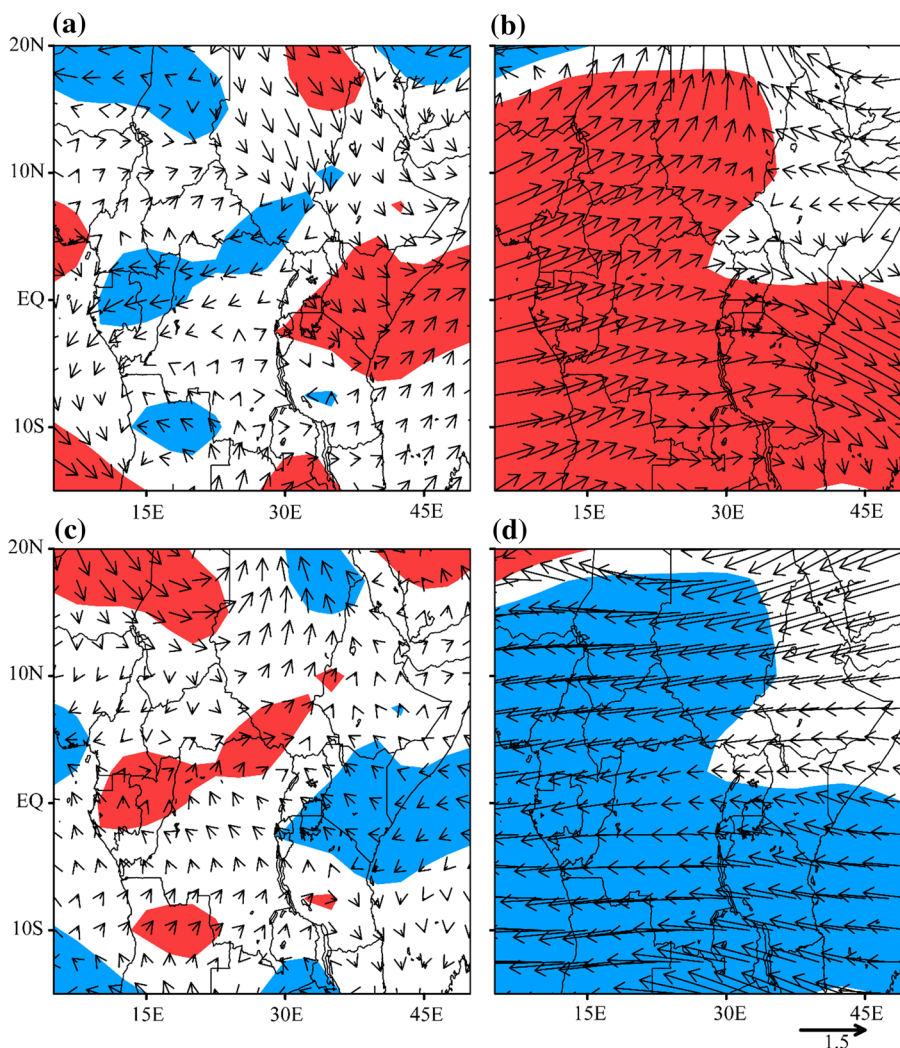
### 3.3 Circulation Anomaly Patterns for Wet and Dry MAM Rainfall

This section looks into concept of circulation anomaly patterns associated with wet and dry events of boreal spring rainfall.

#### 3.3.1 Wind and Moisture Flux Patterns

Figure 5 displays wind circulation anomaly during wet years (1977, 1981, 1988, 2002, 2003 and 2010) and dry years (1973, 1976, 1984, 1993, 2000 and 2009) at 850 hPa and 200 hPa, respectively. During wet condition, there exists an enhanced significant low-level north westerly convergence emerging from Sudan and Ethiopia all the way to central and south-eastern Kenya (Fig. 5a). This is accompanied with strong north-westerly wind anomalies in the upper level which favors an upper level divergence (Fig. 5b). The northwesterly wind flow at low-level flow towards the study area in Fig. 5a has a devastating impact on the low-level

**Fig. 5** Composite analysis of wind anomaly at **a** 850 hPa and **b** 200 hPa for wet years while dry years at; **c** 850 hPa and **d**. The shaded area is significant at significance level of  $\alpha=0.05$



moisture flux transport from Sudan and Ethiopia to the study area where it converges (Fig. 6a). Having sufficient moisture coupled with low-level convergence over the study area, it leads to ascending motion and enhanced convection which later favors anomalous rainfall (anomalous wet condition). Dry years on the other hand exhibit weak easterly divergence at low level over central and southern part of the study area (Fig. 5c) coupled with decelerating easterly anomalies in the upper level (Fig. 5d). There is suppression of moisture flux transport from the Ethiopia and Sudan towards the country (Fig. 6b). With low-level divergence and inadequate influx of low-level moisture over the study domain, it is obvious that the convection will be suppressed leading to less rainfall and dry condition.

### 3.3.2 Movement of the Pressure Systems

During wet conditions, the Arabian sub-tropical high pressure cell seems to intensify with an inland movement centered at 13°E and 23°N (Fig. 7a). On the other hand, the Mascarene High (MH) weakened significantly. An overall effect of the strengthened and relaxed respective pressure systems helps to position the Intertropical Convergence Zone (ITCZ) over the study domain. This enhances the confluent of northwesterly moist wind from Sudan and Ethiopia to central and southern Kenya as noted earlier (Figs. 5a, 6a). Contrary with the wet years, the Arabian high relaxed while the MH intensifies (Fig. 7b). The strengthened MH causes the ridging high to extent along the Kenyan coast, thereby pushing the ITCZ away from the study domain while

**Fig. 6** The total moisture flux convergence ( $10^{-4} \text{ g kg}^{-1} \text{ s}^{-1}$ ), where positive values represent positive moisture flux convergence

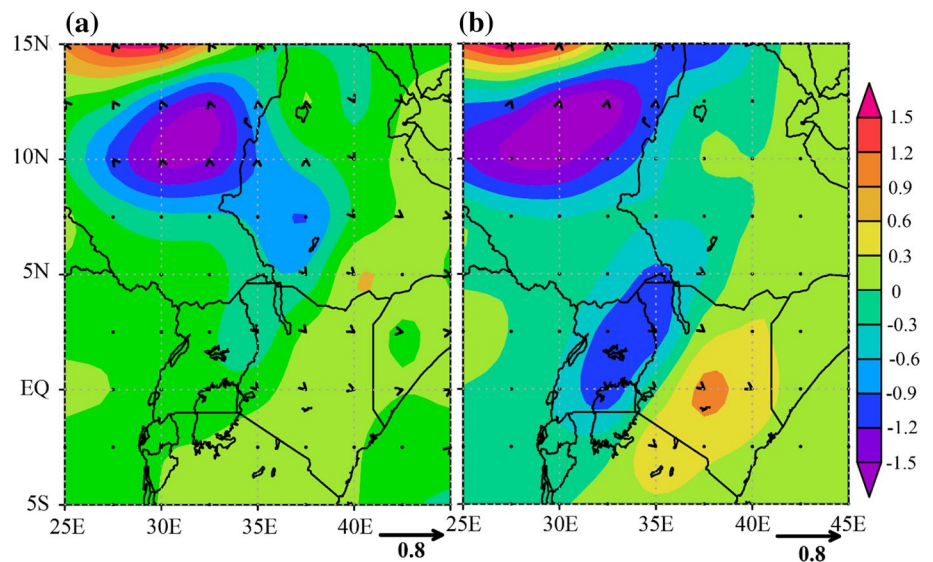
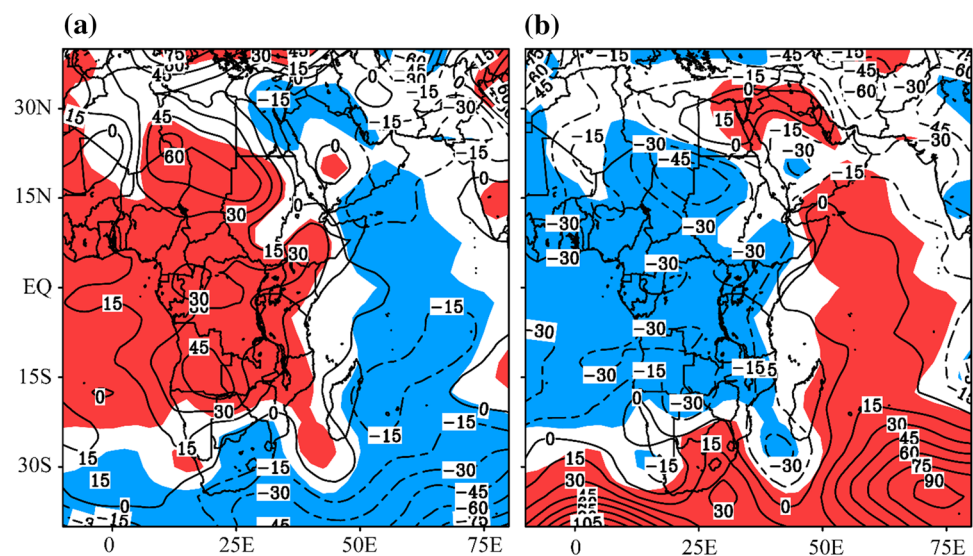


**Fig. 7** Mean sea level pressure anomalies during **a** wet years and **b** dry years. The shaded area is significant at significance level of  $\alpha=0.05$





accelerating weak easterly wind anomalies towards the study area (Fig. 5c).

### 3.3.3 Vertical Velocity and Velocity Potential

The composite vertical cross-section of vertical velocity anomaly at fixed longitude for the wet and dry years is presented in Fig. 8. During wet years (Fig. 8a), there are negative values of vertical velocity from low to high levels over the central to southern region of the country which favors strong rising motion and is suitable for convection and enhanced precipitation. However, the northern part is influenced by positive vertical velocity anomalies at low levels and negative vertical velocity at mid to high levels of the study area. Dry years depict positive vertical velocity anomalies from low to high levels over the central to southern region of the country which favors strong subsidence motion (Fig. 8b). The northern part is influenced by negative (positive) anomalies at low (mid to high) levels of the study area which implies the fact that only shallow uplift persists over the northern part of the country, while the remaining areas experienced subsidence motion and less rainfall.

Figures 9 and 10 represent the composite velocity potential and divergent/convergent wind anomalies during the wet and dry years. It is, however, noted that years with wet conditions in the low levels characterize positive velocity potential anomalies and wind convergence across East African region centered at 70°E and 0° (Fig. 9a). The low-level wind convergence is accompanied by negative velocity potential and wind divergence at higher levels (Fig. 9b), which reposition the ascending limb of local Indian Walker Circulation. Following the positioning of the rising branch of the Walker circulation near the study area, it enhances convection within the locality, accompanied with anomalous wet condition. Dry conditions area is characterized by the descending limb

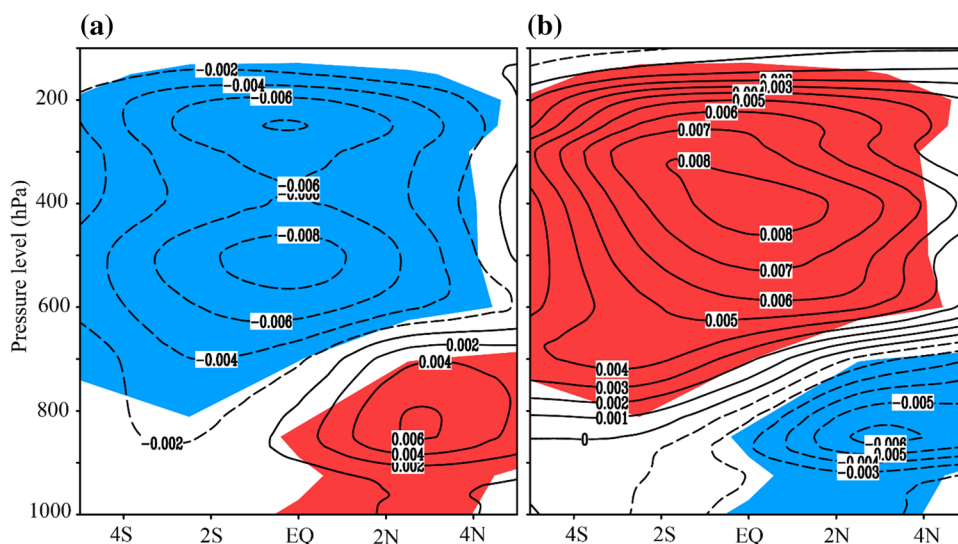
of the local Indian Ocean Walker circulation at 72°E and 8°S (Fig. 10a) with negative velocity potential and wind divergence at low level while positive velocity potential and wind convergence at higher levels (Fig. 10b).

### 3.4 Sea surface Temperature and Outgoing Long-wave Radiation Anomalies

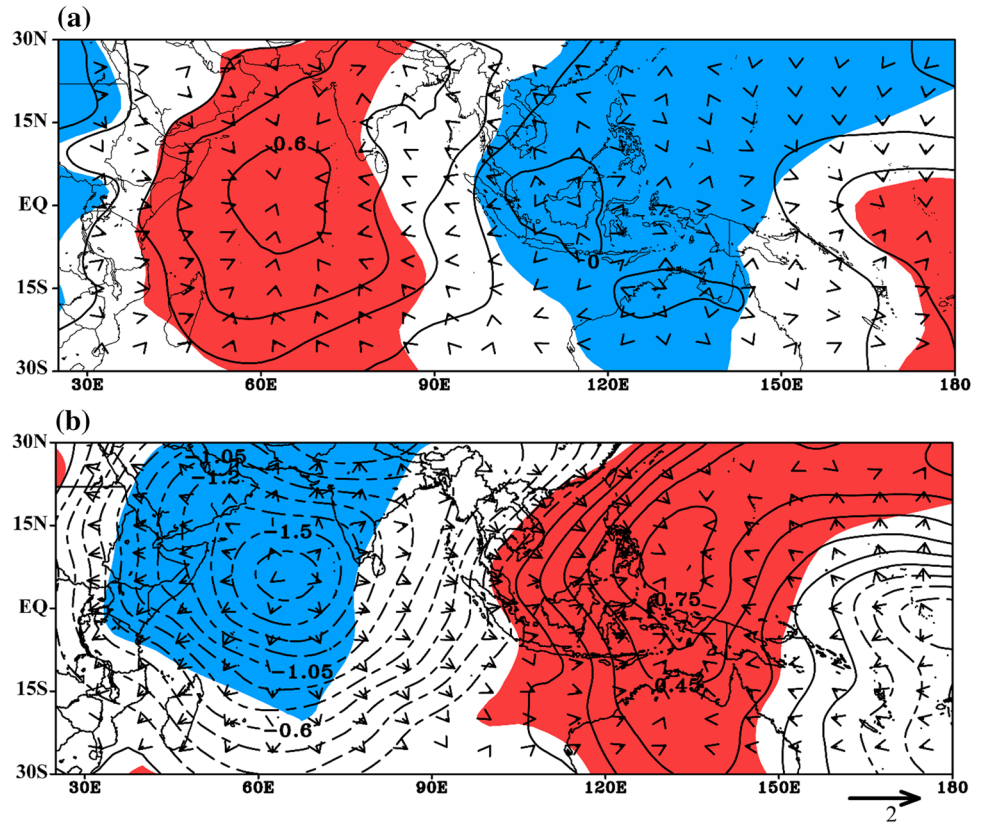
In an attempt to understand the causes of the circulation anomalies and influencing factors responsible for variability of the MAM rainfall, a further investigation of SST anomaly was conducted. The SST plays an important role in the studies of air-sea exchange and circulation patterns. On the inter-annual, seasonal and annual scales, Indian Ocean (IO), Pacific Ocean (PO) and Atlantic Ocean (AO) are known to influence rainfall over EA (Black et al. 2003; Saji and Yamagata 2003; Behera et al. 2005). Predictability of climatic conditions in the regions, hence, depends on accurate analysis of SST patterns and trends. Figure 11 presents the composite SST anomalies during wet/dry years during MAM of 1971–2010.

During wet years (Fig. 11a), the central and sub-tropical IO, western equatorial PO and north-eastern AO characterizes warm SST anomalies while cold SST anomalies are observed over the respective areas with dry years (Fig. 11b). In this study, we extend our analysis on the outgoing long-wave radiation (OLR) aiming at understanding the existing relationship between the SSTA and the OLR. Figure 12a represents the composite OLR pattern anomalies at low level (850 hPa) during wet years. There are strong negative OLR anomalies over the central IO during wet condition while positive anomalies are revealed over the same area during dry condition (Fig. 12b). The central and sub-tropical IO with negative OLR anomalies for wet years means stronger than normal convection activities there, which are

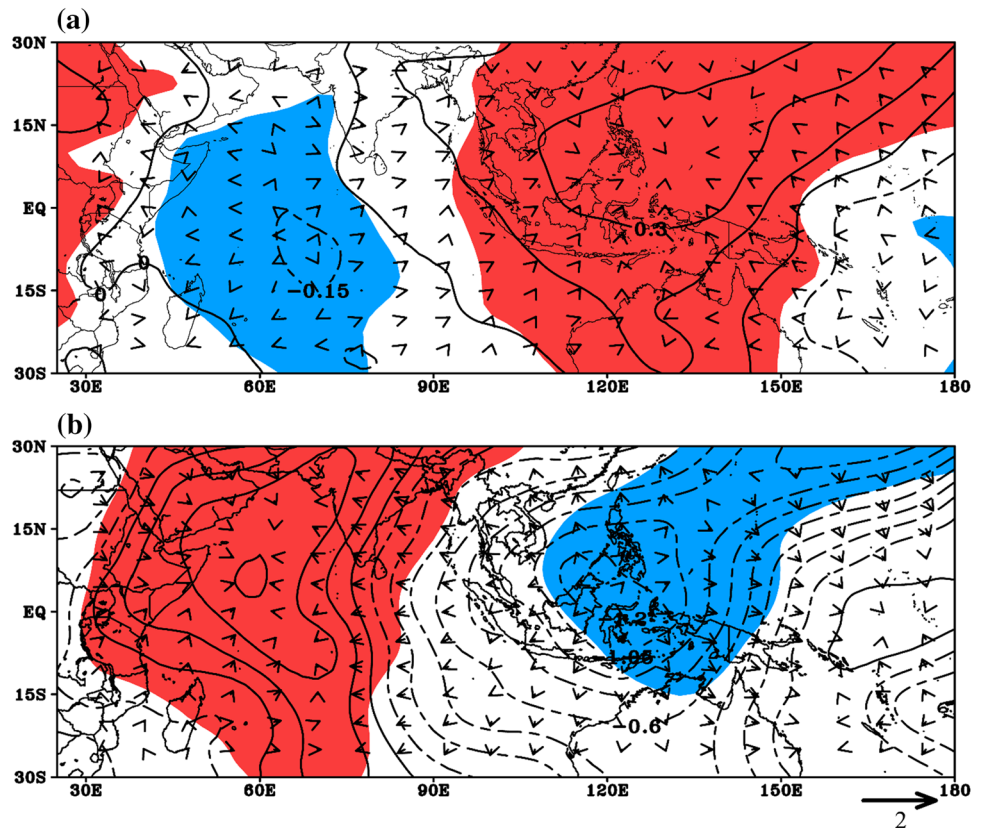
**Fig. 8** Vertical Velocity anomalies during **a** wet years and **b** dry years at fixed longitude [34°E]. Negative (positive) values indicate upward (downward) motion. Contour interval is 0.003 and units are in  $\text{Pas}^{-1}$ . The shaded area are significant at significance level of  $\alpha = 0.05$



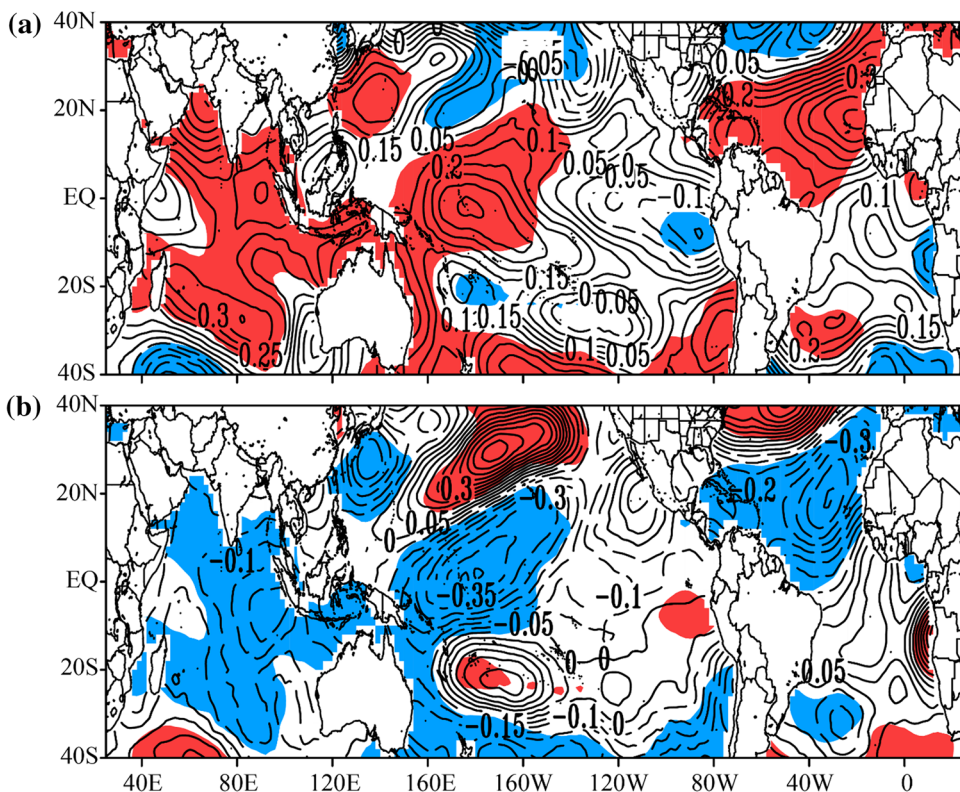
**Fig. 9** Velocity potential and divergent winds for wet years at; **a** 850 hPa and **b** 200 hPa. The shaded area is significant at significance level of  $\alpha=0.05$



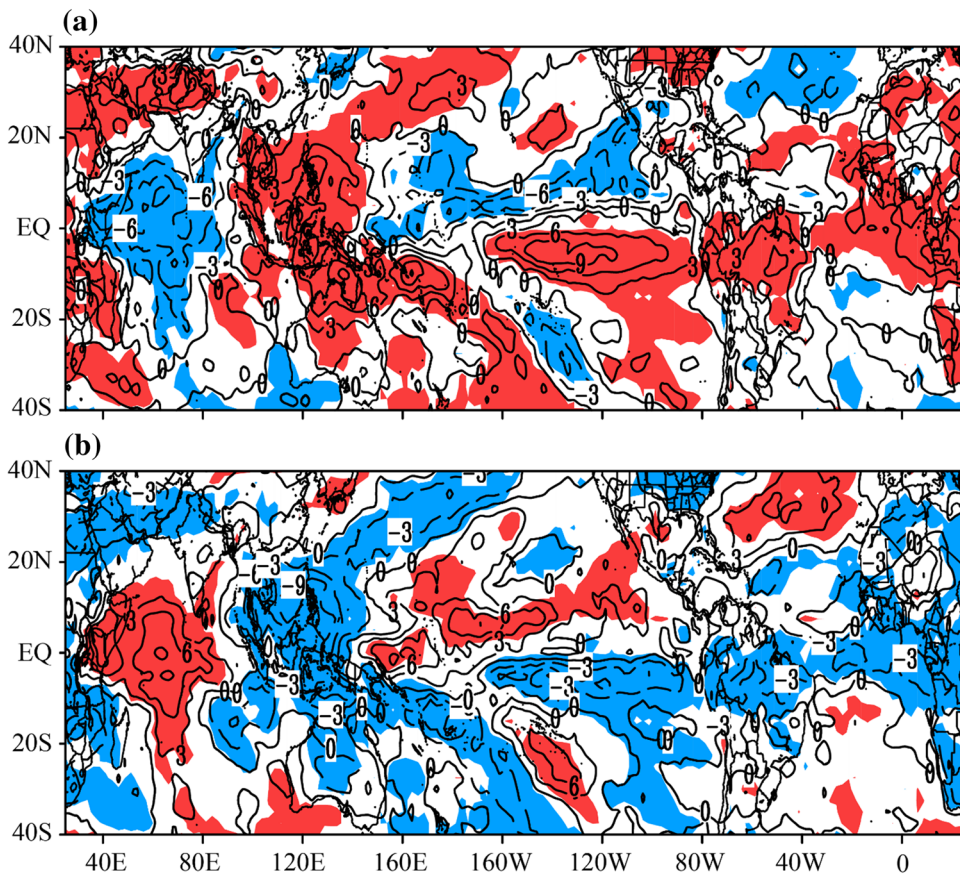
**Fig. 10** Velocity potential and divergent winds for dry years at; **a** 850 hPa and **b** 200 hPa. The shaded area is significant at significance level of  $\alpha=0.05$



**Fig. 11** SST anomaly ( $0^{\circ}\text{C}$ ) during **a** wet years and **b** dry years. The shaded area is significant at significance level of  $\alpha=0.05$



**Fig. 12** The composite OLR ( $\text{Wm}^{-2}$ ) anomaly fields during **a** wet years and **b** dry years. The shaded area is significant at significance level of  $\alpha=0.05$



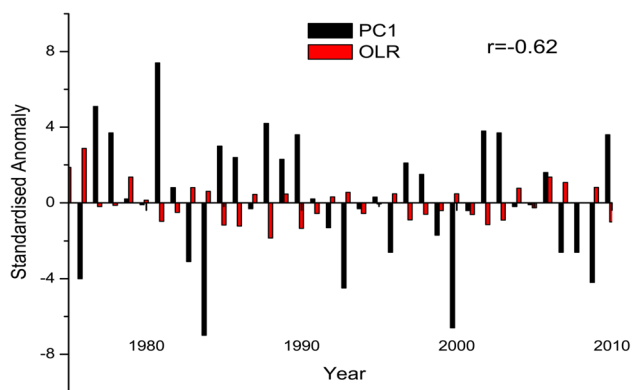


**Fig. 13** The inter-annual variability of mean MAM rainfall and OLR indices averaged over 45°E–80°E and 10°S–10°N of the Indian Ocean during 1971–2010

corresponding the rising branch of the Walker circulation near the study area. We, therefore, extract and normalize the OLR from the central Indian Ocean in an area marked 45°E–80°E and 10°S–10°N. The index from this area was further correlated with PC1 of the dominant mode for the MAM rainfall. The results reveal a reasonable association between MAM rainfall and OLR with a negative correlation coefficient of  $-0.62$ . The negative correlation indicates that the inter-annual variation of the MAM rainfall and OLR is in an opposite phase to the other (Fig. 13) and, hence, more convection (i.e., less mean OLR) and enhanced rainfall over the study domain. This is because water vapor from the Indian Ocean is being advected to the region of convection, which rises (cools) and results in more precipitation.

## 4 Conclusions

This study investigated circulations associated with variations of MAM rainfall anomalies over Kenya during the period 1971–2010. The MK and EOF statistical methods were applied in the analysis. On trend analysis, MAM rainfall revealed an insignificant decreasing trend. The first three EOF modes of MAM rainfall accounted for 59% of variability. EOF1 accounted for the highest variability and consequently considered as the dominant mode and used for further analyses. The years (1977, 1981, 1988, 2002, 2003 and 2010) were identified as wet years, while (1973, 1976, 1984, 1993, 2000 and 2009) constituted the dry years. Analysis of the anomalous years with respect to the different variables showed the local wet (dry) years were associated with convergence (divergence) in the lower troposphere (850 hPa) and divergence (convergence) at the upper level (200 hPa). There is a negative correlation coefficient between MAM rainfall and OLR deducing an opposite phases which

indicate more convection resulting in enhanced rainfall over the study domain.

The study reveals that the circulation anomalies associated with the dry years are opposite to those in wet years and SSTAs in the central and sub-tropical IO are closely related to MAM rainfall over Kenya. SSTAs accompanying with OLR anomalies may lead to anomalous rising branch of the Walker circulation and then influence the MAM rainfall in Kenya. In this paper, we only examine the possible relationship between the IO SSTAs/OLR and the MAM rainfall over Kenya. An open question needing further study is how the SSTAs in the IO influence the circulations and then the MAM rainfall over Kenya. Further work based on numerical simulations is required to gain more insights on the physical mechanisms responsible for the observed linkage and assess the relative contribution of each individual system to the MAM rainfall.

**Acknowledgement** The authors express gratitude to Nanjing University of Information Science and Technology (NUIST) for setting up a conducive learning environment. The work described in this paper is supported by National Science and Technology Support Program of China (2015BAC03B02) and the Priority Academic Program Development of Jiangsu Higher Education Institutions (PAPD) of China. The authors are grateful to the anonymous reviewers for their inputs that tremendously improved the quality of manuscript. Special appreciation goes to all data centers that provided the data sets used in the study.

## Compliance with ethical standards

**Conflict of interest** On behalf of all authors, the corresponding author states that there is no conflict of interest.

## References

- Araghi A, Mousavi-Baygi M, Adamowski J (2016) Detection of trends in days with extreme temperatures in Iran from 1961 to 2010. *Theor Appl Climatol* 125:213–225. <https://doi.org/10.1007/s00704-015-1499-6>
- Awange JL, Aluoch J, Ogallo LA, Omulo M, Omondi P (2007) Frequency and severity of drought in the Lake Victoria region (Kenya) and its effects on food security. *Clim Res* 33:135–142. <https://doi.org/10.3354/cr033135>
- Ayugi BO, Wang W, Chepkemoi D (2016) Analysis of spatial and temporal patterns of rainfall variations over Kenya. *Environ Earth Sci* 6:69–83
- Behera SK, Luo J-J, Masson S, Delecluse P, Gualdi S, Navarra A, Yamagata T (2005) Paramount impact of the Indian Ocean dipole on the East African short rains: a CGCM study. *J Clim* 18:4514–4530. <https://doi.org/10.1175/JCLI3541.1>
- Beri GC (2005) *Business statistics*, 2nd edn. Tata McGraw-Hill Publisher, New York, pp 312–340
- Bisai D, Chatterjee S, Khan A, Barman NK (2014) Long term temperature trend and change point: a statistical approach. *J Atmos Clim Chang* 1:1–12. <https://doi.org/10.15764/ACC.2014.01004>
- Black E, Slingo JM, Sperber KR (2003) An observational study of the relationship between excessively strong short rains in

- coastal East Africa and Indian Ocean SST Mon. *Weather Rev* 131:74–94. <https://doi.org/10.1175/1520-0493>
- Black E, Tarnavsky E, Greatrex, H, Maidment R, Mookerjee A, Quaipe T, Price J (2015) Exploiting satellite-based rainfall for weather index insurance: the challenges of spatial and temporal aggregation. In: First international electronic conference on remote sensing, 22 Jun–5 Jul 2015. (vol 1: f002). <https://doi.org/10.3390/ecrs-1-f002>
- Boiyo R, Kumar KR, Zhao T, Bao Y (2016) Climatological analysis of aerosol optical properties over East Africa observed from space-borne sensors during 2001–2015. *Atmos Environ* 152:298–313. <https://doi.org/10.1016/j.atmosenv>
- Bowden R (2007) Kenya, 2nd edn. Evan Brothers, London
- Brass W, Jolly CL (eds) (1993) Population dynamics of Kenya. National Academy Press, Washington, p 183
- Camberlin P, Okoola RE (2003) The onset and cessation of the ‘long rains’ in eastern Africa and their interannual variability. *Theor Appl Climatol* 54:43–54. <https://doi.org/10.1007/s00704-002-0721-5>
- Camberlin P, Janicot S, Pocard I (2001) Seasonality and atmospheric dynamics of the teleconnection between African rainfall and tropical sea-surface temperature: Atlantic vs ENSO. *Int J Climatol* 21:973–1005. <https://doi.org/10.1002/joc.673>
- Clark CO, Webster PJ, Cole JE (2003) Interdecadal variability of the relationship between the Indian Ocean zonal mode and East African coastal rainfall anomalies. *J Clim* 16:548–554. [https://doi.org/10.1175/1520-0442\(2003\)016%3C0548:IVOTR%3E2.0.CO;2](https://doi.org/10.1175/1520-0442(2003)016%3C0548:IVOTR%3E2.0.CO;2)
- Cook KH, Vizy EK (2013) Projected changes in east african rainy seasons. *J Climate* 26:5931–5948. <https://doi.org/10.1175/JCLI-D-12-00455.1>
- Daron JD (2014) Regional Climate Messages: East Africa. Scientific report from the CARIAA Adaptation at Scale in Semi-Arid Regions (ASSAR) Project, December 2014
- Funk C, Hoell A, Shukla S, Bladé I, Liebmann B, Roberts JB, Husak G (2014) Predicting East African spring droughts using Pacific and Indian Ocean sea surface temperature indices. *Hydrol Earth Syst Sci* 18:4965–4978. <https://doi.org/10.5194/hess-18-4965-2014>
- Gajbhiye S, Meshram C, Mirabbasi R, Sharma SK (2016) Trend analysis of rainfall time series for Sindh river basin in India. *Theor Appl Climatol* 125:593–608. <https://doi.org/10.1007/s00704-015-1529-4>
- Gichangi EM, Gatheru M, Njiru EN, Mungube EO, Wambua JM, Wamuongo JW (2015) Assessment of climate variability and change in semi-arid eastern Kenya. *Clim Change* 130:287–297. <https://doi.org/10.1007/s10584-015-1341-2>
- Hastenrath S, Polzin D, Mutai C (2011) Circulation mechanisms of kenya rainfall anomalies. *J Clim* 24:404–412. <https://doi.org/10.1175/2010JCLI3599.1>
- Indeje M, Semazzi FHM, Ogallo LJ (2000) ENSO signals in East African rainfall seasons. *Int J Climatol* 20:19–46. [https://doi.org/10.1002/\(SICI\)1097-0088\(200001\)20:1%3c19:AID-JOC449%3e3.0.CO;2-0](https://doi.org/10.1002/(SICI)1097-0088(200001)20:1%3c19:AID-JOC449%3e3.0.CO;2-0)
- IPCC (2013) Climate change 2013: the physical science basis. Contribution of Working Group I to the Fifth Assessment Report of the Intergovernmental Panel on climate change [Stocker TF, Qin D, Plattner G-K, Tignor M, Allen SK, Boschung J, Nauels A, Xia Y, Bex V, Midgley PM (eds.)]. Cambridge University Press, Cambridge, pp 1535
- Kendall MG (1975) Rank correlation methods, 4th edn. Griffin, London, p 202
- Kerandi N, Arnault J, Laux P, Wagner S, Kitheka J, Kunstmann H (2018) Joint atmospheric-terrestrial water balances for East Africa: a WRF-Hydro case study for the upper Tana River basin. *Theor Appl Climatol* 131:1337–1355. <https://doi.org/10.1007/s00704-017-2050-8>
- Liebmann B, Hoerling MP, Funk C, Bladé I, Dole RM, Allured D, Eischeid JK (2014) Understanding recent eastern Horn of Africa rainfall variability and change. *J Clim* 27:8630–8645. <https://doi.org/10.1175/JCLI-D-13-00714.1>
- Liuzzo L, Bono E, Sammartano V, Freni G (2016) Analysis of spatial and temporal rainfall trends in Sicily during the 1921–2012 period. *Theor Appl Climatol* 126:113–129. <https://doi.org/10.1007/s00704-015-1561-4>
- Lorenz EN (1956) Empirical orthogonal functions and statistical weather prediction. Technical Report Statistical Forecast Project Report 1 Department of Meteorology MIT 49
- Maidment RI, Allan RP, Black E (2015) Recent observed and simulated changes in rainfall over Africa. *Geophys Res Lett* 42:8155–8164. <https://doi.org/10.1002/2015GL065765>
- Makkonen L (2006) Plotting positions in extreme value analysis. *J Clim Appl Meteorol* 45:334–340
- Manatsa D, Morioka Y, Behera SK, Matarira CH, Yamagata T (2014) Impact of Mascarene high variability on the East African ‘short rains’. *Clim Dyn* 42:1259–1274. <https://doi.org/10.1007/s00382-013-1848-z>
- Mann HB (1945) Nonparametric tests against trend. *Econometrica* 13:245–259
- Marshall M, Funk C, Michaelsen J (2012) Examining evapotranspiration trends in Africa. *Clim Dyn* 38:1849–1865. <https://doi.org/10.1007/s00382-012-1299-y>
- Meng X, Zhang S, Zhang Y, Wang C (2013) Temporal and spatial changes of temperature and precipitation in Hexi Corridor during 1955–2011. *J Geogr Sci* 23:653–667. <https://doi.org/10.1007/s11442-013-1035-5>
- Ministry of Agriculture (2009) Agricultural Sector Development Strategy, ASDS (<http://www.kilimo.go.ke>)
- Mouhamed L, Traore SB, Alhassane A, Sarr B (2013) Evolution of some observed climate extremes in the West African Sahel. *Weather Clim Extremes* 1:19–25. <https://doi.org/10.1016/j.wace.2013.07.005>
- Nicholson SE (2008) The intensity, location and structure of the tropical rainbelt over west Africa as factors in interannual variability. *Int J Climatol* 28:1775–1785. <https://doi.org/10.1002/joc.1507>
- Nicholson SE (2016) An analysis of recent rainfall conditions in eastern Africa. *Int J Climatol* 36:526–532. <https://doi.org/10.1002/joc.4358>
- Nicholson SE, Selato JC (2000) The influence of La Nina on Africa rainfall. *Int J Climatol* 20:1761–1776
- Nicholson SE, Leposo D, Grist J (2001) The relationship between El Niño and drought over Botswana. *J Clim* 14:323–335. [https://doi.org/10.1175/1520-0442\(2001\)014%3C0323:TRBEN%3E2.0.CO;2](https://doi.org/10.1175/1520-0442(2001)014%3C0323:TRBEN%3E2.0.CO;2)
- Ogwang BA, Chen H, Li X, Gao C (2014) The influence of topography on East African October to December climate: sensitivity experiments with RegCM4. *Adv Meteorol*. <https://doi.org/10.1155/2014/143917>
- Ogwang BA, Chen H, Tan G, Ongoma V, Ntwali D (2015a) Diagnosis of East African climate and the circulation mechanisms associated with extreme wet and dry events: a study based on RegCM4. *Arab J Geosci* 8:10255–10265. <https://doi.org/10.1007/s12517-015-1949-6>
- Ogwang BA, Ongoma V, Li X, Ogou FK (2015b) Influence of mascarene high and Indian Ocean dipole on East African extreme weather events. *Geogr Pannon* 19:64–72
- Okoola RE (1999) Midtropospheric circulation patterns associated with extreme dry and wet episodes over equatorial Eastern Africa during the Northern Hemisphere spring. *J Clim Appl Meteorol Climatol* 38:1161–1169. [https://doi.org/10.1175/1520-0450\(1999\)038%3c1161:MCPAWE%3e2.0.CO;2](https://doi.org/10.1175/1520-0450(1999)038%3c1161:MCPAWE%3e2.0.CO;2)
- Ongoma V, Chen H (2017) Temporal and spatial variability of temperature and precipitation over East Africa from 1951 to 2010.

- Meteorol Atmos Phys 129:131–144. <https://doi.org/10.1007/s00703-016-0462-0>
- Ongoma V, Muthama JN, Gitau W (2013) Evaluation of urbanization influences on urban temperature of Kenyan cities. *Glob Meteorol*. <https://doi.org/10.4081/gm.2013.e1>
- Ongoma V, Guirong T, Ogwang BA, Ngarukiyimana JP (2015) Diagnosis of seasonal rainfall variability over East Africa: a case study of 2010–2011 drought over Kenya. *Pak J Meteorol* 11:13–21
- Ongoma V, Chen H, Gao C, Sagero PO (2017) Variability of temperature properties over Kenya based on observed and reanalyzed datasets. *Appl Climatol, Theor*. <https://doi.org/10.1007/s00704-017-2246-y>
- Ongoma V, Chen H, Gao C (2018a) Projected change in mean rainfall and temperature over East Africa based on CMIP5 models. *Int J Climatol* 38:1375–1392. <https://doi.org/10.1002/joc.5252>
- Ongoma V, Chen H, Gao C, Nyongesa AM, Polong F (2018b) Future changes in climate extreme over equatorial East Africa based on CMIP5 multimodel ensemble. *Nat Hazards* 90:901–920. <https://doi.org/10.1007/s11069-017-3079-9>
- Owiti Z, Ogallo LA, Mutemi J (2008) Linkages between the Indian Ocean Dipole and east African seasonal rainfall anomalies. *J Kenya Meteorol Soc* 2:3–17
- Partal T, Kahya E (2006) Trend analysis in Turkish precipitation data. *Hydrol Process* 20:2011–2026. <https://doi.org/10.1002/hyp.5993>
- Peel MC, Finlayson BL, McMahon TA (2007) Updated world map of the Koppen-Geiger climate classification. *Hydrol Earth Syst Sci* 11:1633–1644
- Saji NH, Yamagata T (2003) Structure of SST and surface wind variability during Indian Ocean Dipole mode events: COADS observations. *J Clim* 16:2735–2751. [https://doi.org/10.1175/1520-0442\(2003\)016%3c2735:SOSASW%3e2.0.CO;2](https://doi.org/10.1175/1520-0442(2003)016%3c2735:SOSASW%3e2.0.CO;2)
- Schreck CJ, Semazzi FHM (2004) Variability of the recent climate of eastern Africa. *Int J Climatol* 24:681–701. <https://doi.org/10.1002/joc.1019>
- Stern DI, Gething PW, Kabaria CW, Temperley WH, Noor AM, Okiro EA, Hay SI (2011) Temperature and malaria trends in highland East Africa. *PLoS ONE* 6:4–12. <https://doi.org/10.1371/journal.pone.0024524>
- University of East Anglia Climatic Research Unit, Harris I, Jones PD (2014) CRU TS3.22: Climatic Research Unit (CRU) Time-Series (TS) Version 3.22 of high resolution gridded data of month-by-month variation in climate (Jan. 1901– Dec. 2013). NCAS British Atmospheric Data Centre, <http://dx.doi.org/10.5285/18BE23F8-D252-482D-8AF9-5D6A2D40990C>. Accessed 10 May 2017
- Yang W, Seager R, Cane MA, Lyon B (2014) The East African long rains in observations and models. *J Clim* 27:7185–7202. <https://doi.org/10.1175/JCLI-D-13-00447.1>
- Yang W, Seager R, Cane MA, Lyon B (2015) The annual cycle of East African precipitation. *J Clim* 28:2385–2404. <https://doi.org/10.1175/JCLI-D-14-00484.1>